Temperature variability of the Iberian Range since 1602 inferred from tree-ring records

E. Tejedor[1,2,3], M.A. Saz[1,2], J.M. Cuadrat[1,2], J. Esper[3], M. de Luis[1,2]

[1]{University of Zaragoza, 50009 Zaragoza, Spain}

[2]{Environmental Sciences Institute of the University of Zaragoza }

[3]{Department of Geography, Johannes Gutenberg University, 55099 Mainz, Germany}

Correspondence to: E. Tejedor (etejedor@unizar.com)

Abstract

Tree-rings are an important proxy to understand the natural drivers of climate variability in the Mediterranean basin and hence to improve future climate scenarios in a vulnerable region. Here, we compile 316 tree-ring width series from 11 conifer sites in the western Iberian Range. We apply a new standardization method based on the trunk basal area instead of the tree cambial age to develop a regional chronology which preserves high to low frequency variability. A new reconstruction for the 1602-2012 period correlates at -0.78 with observational September temperatures with a cumulative mean of the 21 previous months over the 1945-2012 calibration period. The new $IR2T_{max}$ reconstruction is spatially representative for the Iberian Peninsula and captures the full range of past Iberian Range temperature variability. Reconstructed long-term temperature variations match reasonably well with solar irradiance changes since warm and cold phases correspond with high and low solar activity, respectively. In addition, some annual temperatures downturns coincide with volcanic eruptions with a three year lag.

1 Introduction

The IPCC report (IPCC, 2013) highlighted a likely increase of average global temperatures in upcoming decades, and pointed particularly to the Mediterranean basin, and therefore in the

Iberian Peninsula (IP), as a region of substantial modelled temperature changes. The Mediterranean area is located in the transitional zone between tropical and extra-tropical climate systems, characterized by a complex topography and high climatic variability (Hertig and Jacobeit 2008). Taking into account these features, even relatively minor modifications of the general circulation, i.e. a shift in the location of sub-tropical high pressure cells, can lead to substantial changes in Mediterranean climate (Giorgi and Lionello 2008), making the study area a potentially vulnerable region to anthropogenic climatic changes by anthropogenic forces, i.e. increasing concentrations of greenhouse gases (Lionello et al., 2006a; Ulbrich et al., 2006)

Major recent efforts have been made in understanding trends in temperatures throughout the IP over the instrumental period (Kenaway et al., 2012; Pena-Angulo et al., 2015; Gonzalez-Hidalgo et al., 2015) and future climate change scenarios (Sánchez et al., 2004; López-Moreno et al., 2014). However, the fact that most of the observational records do not begin until the 1950s (Gonzalez-Hidalgo et al., 2011) is limiting the possibility of investigating the inter-annual to multi-centennial long-term temperature variability. Therefore, it is crucial to explore climate proxy data and develop long-term reconstructions of regional temperature variability to evaluate spatial patterns of climatic change and the role of natural and anthropogenic forcings on climate variations (Büntgen et al., 2005). In the IP, much progress has been made to reconstruct past centuries climate variability, including analysis of documentary evidences for temperature (i.e. Camuffo et al., 2010) and droughts reconstruction (i.e. Barriendos et al. 1997; Cuadrat and Vicente, 2007; Domínguez-Castro et al., 2010). Additionally, progress has been made to further understanding of long-term climate variability of the IP through dendroclimatological studies focussing on drought (Esper et al., 2014; Tejedor et al., 2015) and temperature (Büntgen et al., 2008; Dorado-Liñán et al., 2012, 2014; Esper et al. 2015a). Nevertheless, a high-resolution temperature reconstruction for central Spain is still missing.

Several studies have been made to develop a temperature reconstruction for the Iberian Range (IR) using *Pinus uncinata* tree-ring data (Creus and Puigdefabreas, 1982; Ruiz, 1989). The results, in fact, showed a pronounced inter-annual to century scale chronology variability. However, their main result was a complex growth response function due to a mixed climate signal instead of a temperature reconstruction. Furthermore, Saz (2003) developed a 500-year temperature reconstruction for the Ebro Depression (North of Spain), but this chronology is

based on a reduced number of cores and a standardized methodology that did not retain the medium and low frequency variance.

Here we present the first tree-ring dataset combining samples from three different sources from the eastern IR extending back from the Little Ice Age (1465) to present (2012). The aim of this study is to develop a temperature reconstruction representing the IR, and thereby fill the gap between records located in the northern and southern IP. A new methodology, based on basal area instead of the cambial-age, was applied to preserve high-to-low frequency variance in the resulting chronologies. Furthermore, the relationship between the tree-ring and climate data is reanalysed by adding memory to the climate parameters, since memory effects on tree-ring data are much less acknowledged (Anchukaitis et al., 2012). This analysis is challenging because of the mix of tree species and their unidentified responses to climate. The resulting reconstruction of September maximum temperatures over the past four centuries is compared with latest findings from the Pyrenees and Cazorla, and the relationship with solar and volcanic forcings at inter-annual to multi-decadal timescales.

2 Material and methods

2.1 Site description

We compiled a tree ring network from 11 different sites in the western IR (Table 1) in the province of Soria. Urbión is the most extensive forest of the IP including 120,000 ha between the Burgos and Soria provinces. It has a long forest management tradition. Therefore, all sites are situated at high elevation locations where forests are least exploited and maximum tree age is reached (Fig.1). The altitude of the sampling sites ranges from 1,500 to 1,900 meters above sea level (masl) with a mean of 1,758 masl. These forests belong to the Continental Bioclimatic Belt (Guijarro, 2013) characterized by moderate mean temperatures (9.5°C, Fig.2B) and a large seasonal range including more than 90 frost days and summer heat exceeding 30ºC . Mean annual precipitation for the period 1944-2014 is 927 mm (CRU TS.3 v.23 dataset by Harris et al., 2014) and reaches its maximum during December (Fig. 2AC).

Although scotts pine (*Pinus sylvestris*) is the dominant tree species of the region, other pinaceaes are found such as *Pinus pinaster*, *Pinus nigra* or *Pinus uncinata*. Especially remarkable is occurrence of *Pinus uncinata* growing above 1,900 masl and reaching its

European southern distribution limits in the IR. The lithology of the study area consists of sandstones, conglomerates and lutites.

2.2 Tree ring chronology development

The new dataset is composed by 316 tree-ring width (TRW) series of *Pinus uncinata* (56) and *Pinus sylvestris* (260) located in the western IR (Tab. 1, Fig. 1). The most recent samples were collected during the field campaign in 2013 including old dominant and co-dominant trees with healthy trunks and no sign of human interference. We extracted two core samples from each tree at breast height (1.3 m) when possible, otherwise, we try to avoid compression wood due to steep slopes, compiling a set of 96 new samples from two sites, i.e. the outermost ring is 2012. Core samples were air-dried and glued onto wooden holders and subsequently sanded to ease growth ring identification (Stokes and Smiley 1968). The samples were then scanned and synchronized using CoRecorder software (Larsson 2012) (Cybis Dendrochronology 2014) to identify the position and exact dating of each ring. The tree-ring width was measured, at 0.01 mm precision, using LINTAB table (Rinn 2005). Prior to detrending, COFECHA (Holmes 1983) was used to assess the cross-dating of all measurement series.

An additional set of 95 samples from three sites was provided by the project CLI96-1862 (Creus et al. 1992, Saz 2003) i.e., the outermost rings range from 1992 to 1993. Finally, a set of 125 samples from five sites was downloaded from the International Tree Ring Data Bank (ITRDB, http://www.ncdc.noaa.gov/data-access/paleoclimatology-data/datasets/tree-ring). These data were developed in the 1980s by K. Richter and collaborators, i.e. the outermost rings range from 1977 to 1985.

In order to attempt a climate reconstruction for the western IR from this tree-ring network, we perform an exploratory analysis of the 11 tree-ring sites by creating a correlation matrix of the raw TRW series for each site and the correlation with a composite regional chronology. Calculations are computed for the common period (1842-1977) and for the full period (1465-2012).

2.2.1 Standardization methods

The key concept in dendroclimatology is referred to as the standardization process (Fritts, 1976; Cook et al., 1990) where the aim is to preserve as much of the climate-related

information as possible while removing the non-climatic information from the raw TRW measurements. However, with most of the standardization methods a varying proportion of the low-frequency climatic information is also lost in the process (Grudd, 2008). When the aim is to use tree-ring chronologies as a proxy for climatic reconstructions, an adequate standardization is critical and the best method should preserve high to low frequency variations (Büntgen et al., 2004). It is common practice to calculate a mean value function as the best estimate of the trees' signal at a site (Frank et al., 2006).

We here applied four standardization methods to the 316 TRW measurement series to develop a single tree-ring index chronology. (i) To emphasize inter-decadal and higher frequency variations, each ring width series was fitted with a cubic spline with a 50% frequency response cut off at 67% of the series length (Cook et al., 1990). A bi-weight robust mean was calculated to assemble the ArstanSTD regional chronology. (ii) A residual chronology (ArstanRES) is produced after removing first-order autoregression to emphasize high-frequency variability. (iii) To preserve common inter-decadal and lower frequency variations, Regional Curve Standardization (RCS) was applied (Mitchell, 1967; Briffa et al., 1992, 1996; Esper et al., 2003). RCS is an age-dependent composite method and involves dividing the size of each tree-ring by the value expected from its cambial age. To assemble the chronology, all the series are aligned by cambial age. A single growth function (regional curve, RC) smoothed using a spline function of 10% of the series length is fit to the mean of all age-aligned series. A biweigth robust mean was applied to develop the RCS chronology (RCS). (iv)To preserve high to low frequency variance, we additionally applied a novel standardization method based on the principles of RCS. However, instead of using the cambial age of the trees as the independent variable, we used their sizes, calculated as the square of the basal area of the tree in the year prior to ring formation. Then, a Poisson regression model was used to fit the individual tree-ring widths. Standardized indices were calculated as the ratio between the observed and predicted values, and a biweigth robust mean was used to develop the Basal Area Poisson chronology (BasPois).

To evaluate uncertainty of the mean chronologies running interseries correlations (Rbar) and the express population signal (EPS) were calculated (Wigley et al., 1984). Rbar is a measure of the strength of the common growth 'signal' within the chronology (Wigley et al. 1984; Briffa and Jones, 1990), here calculated in a 50-year window sliding along the chronology.

EPS is an estimate of the chronology's ability to represent the signal strength of a chronology on a theoretical infinite population (Wigley et al., 1984).

2.3 Climatic data, calibration and climate reconstruction

Monthly temperature (mean, maximum, and minimum) and precipitation values from the gridded CRU TS v.3.22 dataset (0.5º resolution) dataset for the period 1945-2012 were used (Harris et al. 2014). The three grid points closest to the tree-ring network were averaged to develop a regional time series (Fig. 1). In addition, we calculate a cumulative monthly mean for each of the four parameters (max., min., mean temperature, and monthly precipitation). The cumulative mean is calculated by adding the months gradually. First the previous month is added, and then further months are included up to 36 previous months. For the calculations we take into account the current and the previous year.

For calibration, we correlated the four chronologies (ArstanSTD, ArstanRES, RCS, and BasPois) with monthly climate data and the cumulative monthly mean derived. However, to be consistent statistically, the two chronologies which highlight high frequency variations, ArstanRES and ArstanSTD, were correlated with the detrended climatic data. To assess the stability of the correlation, we calculated a 30-year moving correlation shifted along 1945-2012 with the cumulative monthly mean from the current and the previous year. In addition, the maximum and minimum differences between the moving correlations were calculated. As a result, the climatic variable chosen for the reconstruction is supported by having the highest moving correlation with the least difference between the maximum and the minimum over the moving correlation period.

A split calibration/verification approach was perform over the periods 1945-1978 and 1979-2012 to evaluate the accuracy of the transfer model considering the following metrics; Pearson's correlation (r), coefficient of determination (r^2), reduction of error (RE), mean square error (MSE), the sign test (Cook et al., 1994) and the Durbin-Watson test (Durbin and Watson, 1951). R is a measure of the linear correlation between the chronology and climatic variable. R^2 indicates how well the data fit a statistical model. An r^2 of 1 indicates that the regression line perfectly fits the data; an r^2 of 0 indicates that there is not fit at all. RE is a measure of shared variance between actual and estimated series and provides sensitive measure of the reliability of a reconstruction (Cook et al., 1994; Akkemik et al., 2005; Büntgen et al., 2008); it ranges from +1 indicating perfect agreement, to minus infinity. MSE

estimates the difference between the modelled and measured while sign test compares the number of agreeing and disagreeing interval trends, from year-to-year, between the observed and reconstructed series (Fritts et al., 1990; Cufar et al., 2008). To verify that there is no autocorrelation in the residuals we perform the Durbin-Watson test. Additionally, a Superposed Epoch Analysis (SEA; Panofsky and Brier, 1958) was performed using dplR (Bunn, 2008) to assess post-volcanic cooling signals in our reconstruction. The approach has been used in studies of volcanic effect on climate (Fischer et al., 2007; D'Arrigo et al., 2009; Esper et al. 2013a, 2013b). The major volcanic events chosen for the analysis were those identified by Crowley (2000).

To transfer the TRW chronology into a temperature reconstruction a linear regression model was used. The magnitude and the spatial extent of the climate signal are evaluated considering the CRU TS v. 3.22 gridded dataset for Europe.

3 Results

The correlation matrix (Fig. 3) shows not only the high inter-correlation between sampling sites and tree species but also the high correlation between each chronology and the regional chronology. The highest correlation is found between *Pinus uncinata* (VIN and CAV) located at the highest altitude. On the other hand, the weakest correlation is found between one of the lowest sites (s006) and the highest (VIN). The mean correlation among all sampling sites is r = 0.51 over the common period (1842-1977) is 0.51, and r = 0.46 over the full period of overlap, revealing a regionally common, external forcing controlling tree growth and justifying the development of a single chronology integrating the data from this IP tree-ring network.

The model (regional curve) of the RCS standardization method and the model of the BasPois method are presented in Fig.4. BasPois model (Fig.4a) indicates a growth of 130 mm when the size of the basal area is near 0 and a growth of 8mm when it reaches the maximum basal area. RCS model (Fig.4b) presents values of 250 mm of growth when the cambial age is 0 with a gradual decline of the growth until the cambial of 450. Cambial age from 500 to 550 has a slight increase in growth most likely derived by low replication regarding trees with this age.

Calibration of the four differently detrended mean chronologies reveals a highly negative correlation with maximum temperatures (Fig. 5). The ArstanRES chronology shows moderate correlations with previous-year September (r = -0.39), and the ArstanSTD chronology correlates at r = -0.56 with September and October temperature of the previous year with a cumulative monthly mean of 21 months. Considering the RCS chronology, the previous-year September signal increases to r = -0.57 with a cumulative monthly mean of 21 months. Finally, the best correlation is revealed for the BasPois chronology reaching r = -0.78 with maximum September temperature of the previous year with a cumulative mean of 21 months, which is, in fact a two year cumulative monthly mean. Even though the signals show the same seasonal patterns among the chronologies, the BasPois record always shows the highest correlations. Accordingly, we used the BasPois chronology for the calibration and reconstruction process.

The final BasPois network chronology (Fig.6) is based on 316 TRW series of *Pinus uncinata* and *Pinus sylvestris* spanning the 1465-2012 period. Since this chronology is derived from only living trees, mean chronology age increases from 47 years in 1966 to 528 in 1465. The mean sensitivity is 0.21, and first-order autocorrelation is 0.83. The inter-series correlation (Rbar) reaches 0.26, and the first principal component explains about 35% of the variance. The network chronology's signal to noise ratio is 48.52, and EPS exceeds 0.85 after 1602, constraining the reconstruction period to 410 years until 2012.

The selection of the best climate parameter to develop the reconstruction is presented in the Figure 7 where correlations between -0.54 and -0.86 representing only the most significant values are shown. Four parameters reveal the highest correlations over the full calibration period: October of the current year with a cumulative monthly mean of 22 months; September of the previous year with a cumulative monthly mean of 20-months; September of the previous year with a cumulative monthly mean of 21months; and October of the previous year with a cumulative monthly mean of 21 months. The stability of the correlation and therefore the consistency of the signal are tested considering the minimum difference between the maximum and minimum correlation (Fig. 7b) over the full running correlation period. The smallest difference (0.24) is reached for September of the previous year with a cumulative monthly mean of 21months. Therefore, this parameter is chosen for the climate reconstruction. According to the 30-year moving correlations, maximum values are reached from 1973-2003 (r = -0.80), whereas the lowest 30-year correlation (r = -0.60) is reached from

1956-1986. In addition, the relationship between September of the previous year with a cumulative monthly mean of 21months is spatially consistent throughout the Iberian Peninsula, reaching into southern France and northern Africa (Fig.11).

The transfer model is validated by the high correlation (r = -0.78) and significant coefficient of determination (r^2 = 0.61) over the full period 1945-2012. Through the split calibration/verification process, considering 1945-1978 and 1979-2012, the temporal robustness was tested revealing highly significant correlations for both periods (r^2=0.41 and r^2=0.55 respectively) and verifying the final reconstruction (Table 2 and Fig. 8). The Durbin-Watson test for the full period (1.45 p<0.0001) indicates no substantial autocorrelation in the residuals. To develop the final reconstruction spanning 1602-2012, we used a lineal regression model over the full period 1945-2012 with maximum temperature of September of the previous year with a cumulative monthly mean of 21months (Eq.1), denominated $IR2T_{max}$:

$$IR2T_{max} = -3.9759 * BasPoisChron + 15.769 (r^2 = 0.61; p < 0.0001) . \quad (1)$$

3.1 $IR2T_{max}$ reconstruction

$IR2T_{max}$ describes 410 years of maximum temperature of September with a cumulative monthly mean of 21-months meaning it has memory of the last two years. Temperature ranges from 13.52ºC (-2.13ºC with respect to the mean) in 1603 to 17.64ºC n (+1.94ºC with respect to the mean) in 2005 (Fig. 9). It is remarkable that the 12 years of the XXI century happen to be within the 25 warmest years. $IR2T_{max}$ covers a part of the Little Ice Age (Grove, 1988) from 1602 to the end of the XIX century. The year-to-year temperature variability is 3.92ºC in the seventeenth century, 2.89ºC in the eighteen century, 3.17ºC in the nineteenth century and 3.07ºC in the twentieth century. The seventeenth and eighteen centuries were the coldest of the reconstruction with 73% and 80% of the years with temperatures below the long-term mean, respectively. On the other hand, the nineteenth and the twentieth centuries were the warmest with 66% and 78% of the years exceeding the mean.

The main driver of the large-scale character of the warm and cold episodes may be changes in the solar activity (Fig.9). The beginning of the reconstruction starts with the end of the Spörer Minimum. The Maunder minimum, from 1645 to 1715 (Luterbach et al., 2001) seems to

cohere with a cold period from 1645 to 1706. In addition, the Dalton minimum from 1796 to 1830, is detected for the period 1810 to 1838. However, a considerably cold period from 1778 to 1798 is not in consonance with a decrease in the solar activity. Four warm periods, 1626-1637, 1800-1809, 1845-1859 and 1986-2012, have been identified to cohere with increased solar activity. Overall, the correlation between the reconstruction and the solar activity is 0.34 ($p < 0.0001$), and increases to r = 0.49 after 11-year low pass filtering the series, thought the degrees of freedom are substantially reduced due to the increase autocorrelation.

The SEA (Fig.10) indicates some impact of volcanic eruptions on the short-term temperature variability within the reconstruction. It shows significance ($p < 0.05$) decrease in September's temperature with a lag of three years.

Figure 11 shows the spatial correlation between the reconstruction and the CRU TS v.3.22 for Europe and northern Africa. High coefficient of determination ($r^2>0.4$, $p < 0.0001$) indicates a robust agreement and spatial extend of the reconstruction over the Iberian Peninsula (IP), especially for the central and Mediterranean Spain. The spatial correlation, however, decreases towards the southwest of the IP and the north of Europe.

4 Discussion and conclusion

Based on a coherent network of 11 tree-ring sites in the IR including 316 TRW series we developed a 410-year maximum September temperature reconstruction. This record is the first climate reconstruction for the IR filling the gap between the temperature reconstructions developed for the north IP (Büntgen et al., 2008; Dorado-Liñán et al., 2012a, Esper et al. 2015a) and for the southern IP (Dorado-Liñán et al, 2014). The $IR2T_{max}$ has been achieved using TRW as well as for the southern IP (Dorado-Liñán et al, 2014). However, for the Pyrenees, MXD (Büntgen et al., 2008, Dorado-Liñán et al., 2012a) or stable isotopes (Esper et al. 2015a) are needed to get skilful records for a temperature reconstruction.

The main statistics used to verify the accuracy of the reconstruction present similar values to those developed for the IP. For instance, the RE coefficient for the period 1945-2012 is 0.56 meaning that the reconstruction has indeed useful skills to develop a reconstruction. A relatively high signal to noise ratio indicates there is meaningful climatic information in the chronology. The mean correlation between sites for the common period (r = 0.51, Fig. 3) reveals substantial agreement between the sites and species. Correlation is strongest among

high elevation sites including the sites VIN and CAV which are both derived from *Pinus uncinata*. The mean chronology, with 35.40% of the first component variance and 48.52 of signal to noise ratio, captures the regional climate signal accurately, which highlights the beauty of regional averages (Briffa et al., 1998).

The original, raw chronology extended over the 1465-2012 period, some 150 years longer than the final reconstruction. However, due to low EPS values prior to 1602, which is related to the low number of samples the final reconstruction was developed for the period 1602-2012.

A novel detrending approach, considering a Basal Area-Poisson model instead of the traditional regional curve (Esper et al. 2003) has certainly improved the skill of the reconstruction and enabled retaining high-to-low frequency climate variance. The traditional approach of using RCS with the mean TRW curve of the age-aligned data only reached correlations with the maximum temperature of September with a cumulative monthly mean of 21months up to r = -0.57, while with the new approach reached r = -0.78.

It is usually difficult to determine the extent to which the effects of environmental factors on tree growth depend on age (genetic control) and/or on size (physiological control), but recent investigations suggest that it is often the size, and not the age, that is important (Mencuccini et al. 2005; Peñuelas 2005). In fact, climate variability is more size-dependent than age or species (De Luis et al., 2009). Hence, the size-based standardization considered here maximizes the common signal. In addition, when combining TRW series from different sites and species, as done here, the heterogeneity in responses might be large. Therefore, size standardization may be a commendable solution to develop unbiased chronologies. Finally, the new method should be tested in other locations since it may help to maximizes responses especially in heterogeneous areas.

The development of climate parameters retaining temperature information of the past 2 years is certainly unusual and distinctive. However, memory effects in TRW data can arise from physiological processes already suggested by Schulman (1956) and Matalas (1962). Moreover, taking into account that TRW growth is conditioned by the storage of starch and sugar in parenchyma ray tissue, the remobilization of carbohydrates from root structures, and the development of needle enduring several growing seasons, influencing the radial increment beyond the instant impact of temperature variability (Pallardy, 2010), led us to add the cumulative monthly mean to the climate parameters. In fact, we demonstrated that the signal

in the study area is magnified with a memory of 21 months from the previous September. Memory effects in TRW data have been also studied regarding the delayed response in TRW (1~5 years) to post volcanic eruptions associated with a decrease in current's year temperature (D'Arrigo et al., 2013, Esper et al., 2014). Thus, developing the two year memory $IR2T_{max}$ allowed us to maintain not only the low frequency signal, highlighting the warm and cold phases, which may be explained by the high correlation with solar activity during 410 years (0.34, p<0.001), but also the high frequency signal, emphasizing the memory effects of the volcanic eruptions in TRW, already studied by Briffa et al. (1998) and recently by Esper et al. (2015b). According to the SEA (Fig.9), the volcanic eruptions have a significance reduction (95% confidence) of September's temperature (-1.98ºC) with a three years lag. However, the $IR2T_{max}$ is already considering the two previous year's temperature, which means the temperature decrease occurred the year after the extreme volcanic event in consistency with (Frank et al., 2007a). The stability of the signal was assessed by a 30-y moving correlation from 1945 to 2012, which shows a better correlation for the period 1979-2012 in agreement with the raise of temperatures observed for last decades which may be limiting TRW growth and therefore magnifying the climate signal. However, the relationship between the chronology and the climate parameter chosen never drops from -0.54 within the calibration period 1945-2012. The negative correlation with maximum temperature of previous September is in concordance with the values detected in Cazorla by Dorado-Liñán et al. 2014. Presumably, a continuous rise in temperatures, as suggested by the IPCC (2013), will trigger an incessant decrease in the tree-ring growth.

Even though the CRU dataset extents the 1901-2013 period, the general distribution of meteorological observatories in Spain did not begin until the mid-twentieth century (Gonzalez-Hidalgo et al. 2011). In fact, the closest instrumental weather station, located in Vinuesa (Fig.1), began in 1945. However, due to the large amount of gaps in the time series, the CRU dataset was used instead for the split calibration/verification approach for the period 1945-2012. The advantages of regional climatic averages were already addressed by Blasing et al. (1981) stating that the average climatic record of the gridded dataset over the study area is representative of the regional climatic conditions, and does not reflect microclimate conditions which may be characteristic of the climatic record at a single station. Tree-ring data might therefore have more variance in common with the regionally averaged climatic record than with the climatic record of the nearest weather station. Generally, studies have shown that the measurements of MXD produce chronologies with an improved climatic signal

(Briffa et al., 2002) as it was revealed for summer temperature reconstructions (Hughes et al., 1984; Büntgen et al. 2008; Matskosvsky and Helama, 2014). However, based on a TRW chronology, it is remarkable the high correlation coefficient for the full calibration period and the CRU dataset (r = -0.78).

Throughout the $IR2T_{max}$ reconstruction we identified the main warm and cold phases (Maunder minimum, Dalton minimum) related with long-term temperature variability generally attributed to changes in cycles of activity (Lean et al., 1995; Lassen et al. 1995; Haigh et al. 2015). In addition, similar cold and warm phases are observed comparing with the Pyrenees (Büntgen et al. 2008) and Cazorla (Dorado-Liñán et al. 2014) reconstructions. However, previously to the Dalton minimum, a warm phase is detected in $IR2T_{max}$ and the Cazorla reconstruction although it is not present in the Pyrenees or in the Alps (Büntgen et al., 2011).

Through the spatial extent and magnitude of the $IR2T_{max}$ reconstruction over Europe it can be acknowledged that the reconstruction is effective and usable for most of the Spanish Iberian Peninsula. Working especially for the central and Mediterranean IP with very high coefficient of determination (r^2>0.4).

Acknowledgements

This study was supported by the Spanish government through the projects ‘CGL2011-28255’, ‘CGL2015-69985’ and the government of Aragon throughout the Program of research groups (group Clima, Cambio Global y Sistemas Naturales, BOA 147 of 18-12-2002) and FEDER funds. Ernesto Tejedor is supported by the government of Aragon with a Ph.D. grant. Fieldwork was carried out in the province of Soria; we are most grateful to its authorities, for supporting the sampling campaign. We are thankful to Klemen Novak, Edurne Martinez, Luis Alberto Longares, and Roberto Serrano for help during fieldwork.

5 References

Akkemik, Ü., Da deviren., N., Aras, A.: A preliminary reconstruction (A.D. 1635–2000) of spring precipitation using oak tree rings in the western Black Sea region of Turkey. Int J Biometeorol 49(5):297–302, 2005.

Anchukaitis, K.J., Breitenmoser, P., Briffa, K.R., Buchwal, A., Büntgen, U., Cook, E.R., D'Arrigo, R.D., Esper, J., Evans, M.N., Frank, D., Grudd, H., Gunnarson, B.E., Hughes, M.K., Kirdyanov, A.V., Körner, C., Krusic, P.J., Luckman, B., Melvin, T.M., Salzer, M.W., Shashkin, A.V., Timmreck, C., Vaganov, E.A., Wilson, R.J.S.: Tree rings and volcanic cooling. Nature Geoscience, 5 (12), pp. 836-837, 2012.

Barriendos, M.: Climatic variations in the Iberian Peninsula during the late Maunder minimum (AD 1675-1715): An analysis of data from rogation ceremonies. Holocene, 7 (1), pp. 105-111, 1997.

Blasing, T. J., D. N. Duvick, and D. C. West: Dendroclimatic calibration and verification using regionally averaged and single station precipitation data, Tree-Ring Bulletin, 41, 37-43, 1981.

Briffa, K.R. and Jones, P.D.: Basic chronology statistics and assessment. In: Methods of Dendrochronology: Applications in the Environmental Sciences (Eds. E.R. Cook and L.A. Kairiukstis), pp.137-152, 1990.

Briffa, K.R., Jones, P.D., Bartholin, T.S., Eckstein, D., Schweingruber, F.H., Karlén, W., Zetterberg, P., Eronen, M.: Fennoscandian summers from ad 500: temperature changes on short and long timescales. Climate Dynamics, 7 (3), pp. 111-119, 1992.

Briffa, K.R., Jones, P.D., Schweingruber, F.H., Osborn, T.J.: Influence of volcanic eruptions on Northern Hemisphere summer temperature over the past 600 years. Nature, 393 (6684), pp. 450-455, 1998.

Briffa, K.R., Osborn, T.J., Schweingruber, F.H., Jones, P.D., Shiyatov, S.G., Vaganov, E.A.: Tree-ring width and density data around the Northern Hemisphere: Part 1, local and regional climate signals. Holocene, 12 (6), pp. 737-757, 2002.

Bunn, A.G.: A dendrochronology program library in R (dplR). Dendrochronologia 26:115–124, 2008.

Büntgen, U., Esper, J., Schmidhalter, M., Frank, D.C., Treydte, K., Neuwirth, B., Winiger, M.: Using recent and historical larch wood to build a 1300-year Valais-chronology. In: Gärtner H, Esper J, Schleser G (eds) TRACE 2: 85-92, 2004.

Büntgen, U., Esper, J., Frank, D.C., Nicolussi, K., Schmidhalter, M.: A 1052-year tree-ring proxy for Alpine summer temperatures. Climate Dynamics, 25 (2-3), pp. 141-153, 2005.

Büntgen, U., Frank, D., Grudd, H., Esper, J.: Long-term summer temperature variations in the Pyrenees. Climate Dynamics, 31 (6), pp. 615-631, 2008.

Camuffo, D., Bertolin, C., Barriendos, M., Dominguez-Castro, F., Cocheo, C., Enzi, S., Sghedoni, M., della Valle, A., Garnier, E., Alcoforado, M.-J., Xoplaki, E., Luterbacher, J., Diodato, N., Maugeri, M., Nunes, M.F., Rodriguez, R.: 500-Year temperature reconstruction in the Mediterranean Basin by means of documentary data and instrumental observations. Climatic Change, 101 (1), pp. 169-199, 2010.

Cook, E.R., Briffa, K., Shiyatov, S., Mazepa, V.: Tree-ring standardization and growth trend estimation. In: Cook ER, Kairiukstis LA (eds), Methods of dendrochronology: applications in the environmental sciences. Kluwer Academic Publishers, Dordrecht, pp 104–162, 1990.

Cook, E.R., Briffa, K.R., Jones, P.D.: Spatial regression methods in dendroclimatology: a review and comparison of two techniques. International Journal of Climatology 14, 379–402, 1994.

Creus, J. and Puigdefabregas, J.: Climatología histórica y dendrocronología de *Pinus uncinata R.* Cuadernos de Investigación Geográfica 2(2): 17-30, 1976.

Creus, J., Puigdefabregas, J.: Climatología histórica y dendrocronología de *Pinus uncinata* R. Cuad Investig Geográfica 2(2):17–30, 1982.

Crowley, T.J.: Causes of climate change over the past 1000 years. Science, 289 (5477), pp. 270-277, 2000.

Čufar, K., de Luis, M., Eckstein, D., Kajfez-Bogataj, L.: Reconstructing dry and wet summers in SE Slovenia from oak tree-ring series. Int J Biometeorol 52:607–615, 2008.

D'Arrigo, R., Wilson, R., Tudhope, A.: The impact of volcanic forcing on tropical temperatures during the past four centuries. Nature Geoscience, 2 (1), pp. 51-56, 2009.

D'Arrigo, R., Wilson, R., Anchukaitis, K. J.: Volcanic cooling signal in tree ring temperature records for the past millennium, J. Geophys. Res. Atmos., 118, 2013.

de Luis, M., Novak, K., Čufar, K., Raventós, J.: Size mediated climate-growth relationships in *Pinus halepensis* and *Pinus pinea*. Trees - Structure and Function, 23 (5), pp. 1065-1073, 2009.

Domínguez-Castro, F., García-Herrera, R., Ribera, P., Barriendos, M.: A shift in the spatial pattern of Iberian droughts during the 17th century. Climate of the Past, 6 (5), pp. 553-563, 2010.

Dorado Liñán, I., Büntgen, U., González-Rouco, F., Zorita, E., Montávez, J.P., Gómez-Navarro, J.J., Brunet, M., Heinrich, I., Helle, G., Gutiérrez, E.: Estimating 750 years of temperature variations and uncertainties in the Pyrenees by tree-ring reconstructions and climate simulations. Climate of the Past, 8 (3), pp. 919-933, 2012.

Dorado Liñán, I., Zorita, E., González-Rouco, J.F., Heinrich, I., Campello, F., Muntán, E., Andreu-Hayles, L., Gutiérrez, E.: Eight-hundred years of summer temperature variations in the southeast of the Iberian Peninsula reconstructed from tree rings. Climate Dynamics, 44 (1-2), pp. 75-93, 2014.

Durbin, J., Watson, G. S.: Testing for Serial Correlation in Least Squares Regression, II. Biometrika 38 (1–2): 159–179, 1951.

El Kenawy, A., López-Moreno, J.I., Vicente-Serrano, S.M.: Trend and variability of surface air temperature in northeastern Spain (1920-2006): Linkage to atmospheric circulation. Atmospheric Research, 106, pp. 159-180, 2012.

Esper. J., Cook, E.R., Krusic, P.J., Peters, K., Schweingruber, F.H.: Tests of the RCS method for preserving low-frequency variability in long tree-ring chronologies. Tree-Ring Research 59, 81-98, 2003.

Esper, J., Büntgen, U., Luterbacher, J., Krusic, P.: Testing the hypothesis of post-volcanic missing rings in temperature sensitive dendrochronological data. Dendrochronologia 13, 216-222, 2013.

Esper, J., Schneider, L., Krusic, P.J., Luterbacher, J., Büntgen, U., Timonen, M., Sirocko, F., Zorita, E.: European summer temperature response to annually dated volcanic eruptions over the past nine centuries. Bulletin of Volcanology 75, 2013.

Esper, J., Düthorn, E., Krusic, P., Timonen, M., Büntgen, U.: Northern European summer temperature variations over the Common Era from integrated tree-ring density records. J. Quat. Sci. 29, 487–494, 2014.

Esper, J., Großjean, J., Camarero, J.J., García-Cervigón, A.I., Olano, J.M., González-Rouco, J.F., Domínguez-Castro, F., Büntgen, U.: Atlantic and Mediterranean synoptic drivers of central Spanish juniper growth. Theoretical and Applied Climatology, 2014.

Esper, J., Konter, O., Krusic, P., Saurer, M., Holzkämper, S., Büntgen, U.: Long-term summer temperature variations in the Pyrenees from detrended stable carbon isotopes. Geochronometria 42, 53-59, 2015.

Esper, J., Schneider, L., Smerdon, J.E., Schöne, B.R., Büntgen, U.: Signals and memory in tree-ring width and density data. Dendrochronologia, 35, pp. 62-72, 2015b.

Fischer, E.M., Luterbacher, J., Zorita, E., Tett, S.F.B., Casty, C., Wanner, H.: European climate response to tropical volcanic eruptions over the last half millennium, Geophys. Res. Lett., 34, L05707, 2007.

Frank, D., Esper, J., Cook, E.R.: On variance adjustments in tree-ring chronology development. In: Heinrich I et al. (Eds.) Tree rings in archaeology, climatology and ecology, TRACE, Vol. 4, 56-66, 2006.

Frank, D., Büntgen, U., Böhm, R., Maugeri, M., Esper, J.: Warmer early instrumental measurements versus colder reconstructed temperatures: shooting at a moving target. Quaternary Science Reviews 26, 3298-3310, 2007a.

Fritts, H.C., Guiot, J., Gordon, G.A., Schweingruber, F.H.: Methods of calibration, verification, and reconstruction. In Methods of Dendrocrhonology, 1990.

Fritts, H.C.: Tree rings and climate. Academic Press, London, 1976.

Giorgi, F., Lionello, P.: Climate change projections for the Mediterranean region, Global and Planetary Change, Volume 63, Issues 2–3, September, Pages 90-104, 2008.

González-Hidalgo, J.C., Brunetti, M., de Luis, M.: A new tool for monthly precipitation analysis in Spain: MOPREDAS database (monthly precipitation trends December 1945 November 2005). International Journal of Climatology, 31 (5), pp. 715-731, 2011.

Gonzalez-Hidalgo, J.C., Peña-Angulo, D., Brunetti, M., Cortesi, N. MOTEDAS: A new monthly temperature database for mainland Spain and the trend in temperature (1951-2010). International Journal of Climatology, 2015.

Grudd, H.: Torneträsk tree-ring width and density ad 500-2004: A test of climatic sensitivity and a new 1500-year reconstruction of north Fennoscandian summers. Climate Dynamics, 31 (7-8), pp. 843-857, 2008.

Guijarro, J.A.: Tendencias de la temperatura en España. En García Legaz, C. y Valero, C. (Coords). Fenómenos meteorológicos adversos en España. AEMET y CCS. Madrid, 2013.

Haigh, J.D., Cargill, P.: The Sun's Influence on Climate, pp. 1-207, 2015.

Harris, I., Jones, P.D., Osborn, T.J., Lister, D.H.: Updated high-resolution grids of monthly climatic observations - the CRU TS3.10 Dataset. International Journal of Climatology, 34 (3), pp. 623-642, 2014.

Hertig, E. and J. Jacobeit: Assessments of Mediterranean precipitation changes for the 21st century using statistical downscaling techniques. International Journal of Climatology 28(8): 1025-1045, 2008.

Holmes, R.L.: Computer-assisted quality control in tree-ring dating and measurement. Tree-Ring Bull 43:69–78, 1983.

Hughes, M.K., Schweingruber, F.H., Cartwright, D., Kelly, P.M.: July-August temperature at Edinburgh between 1721 and 1975 from tree-ring density and width data. Nature, 308 (5957), pp. 341-344, 1984

IPCC, 2013: Climate Change 2013: The Physical Science Basis. Contribution of Working Group I to the Fifth Assessment Report of the Intergovernmental Panel on Climate Change [Stocker, T.F., D. Qin, G.-K. Plattner, M. Tignor, S.K. Allen, J. Boschung, A. Nauels, Y. Xia, V. Bex and P.M. Midgley (eds.)]. Cambridge University Press, Cambridge, United Kingdom and New York, NY, USA, 1535 pp, doi:10.1017/CBO9781107415324.

Larsson, L.A.: CoRecorder&CDendro program. Cybis Elektronik & Data AB. Version 7.6, 2012.

Lassen, K., Friis-Christensen, E.: Variability of the solar cycle length during the past five centuries and the apparent association with terrestrial climate. Journal of Atmospheric and Terrestrial Physics, 57 (8), pp. 835-845, 1995.

Lean, J., Beer, J., Bradley, R.: Reconstruction of solar irradiance since 1610: implications for climate change. Geophysical Research Letters, 22 (23), pp. 3195-3198, 1995.

Lionello, P., Malanotte-Rizzoli, P., Boscolo, R., Alpert, P., Artale, V., Li, L., Luterbacher, J., May, W., Trigo, R., Tsimplis, M., Ulbrich, U., Xoplaki, E.: The Mediterranean climate: An overview of the main characteristics and issues. Developments in Earth and Environmental Sciences, 4 (C), pp. 1-26, 2006a.

López-Moreno, J.I., El-Kenawy, A., Revuelto, J., Azorín-Molina, C., Morán-Tejeda, E., Lorenzo-Lacruz, J., Zabalza, J., Vicente-Serrano, S.M.: Observed trends and future projections for winter warm events in the Ebro basin, northeast Iberian Peninsula. International Journal of Climatology, 34 (1), pp. 49-60, 2014.

Luterbacher, J., Rickli, R., Xoplaki, E., Tinguely, C., Beck, C., Pfister, C., Wanner, H.: The Late Maunder Minimum (1675-1715) - A key period for studying decadal scale climatic change in Europe. Climatic Change, 49 (4), pp. 441-462, 2001.

Luterbacher, J., Xoplaki, E., Casty, C., Wanner, H., Pauling, A., Küttel, M., Rutishauser, T., Brönnimann, S., Fischer, E., Fleitmann, D., Gonzalez-Rouco, F.J., García-Herrera, R., Barriendos, M., Rodrigo, F., Gonzalez-Hidalgo, J.C., Saz, M.A., Gimeno, L., Ribera, P., Brunet, M., Paeth, H., Rimbu, N., Felis, T., Jacobeit, J., Dünkeloh, A., Zorita, E., Guiot, J., Türkes, M., Alcoforado, M.J., Trigo, R., Wheeler, D., Tett, S., Mann, M.E., Touchan, R., Shindell, D.T., Silenzi, S., Montagna, P., Camuffo, D., Mariotti, A., Nanni, T., Brunetti, M., Maugeri, M., Zerefos, C., Zolt, S.D., Lionello, P., Nunes, M.F., Rath, V., Beltrami, H., Garnier, E., Ladurie, E.L.R.: Chapter 1 Mediterranean climate variability over the last centuries: A review, 2006.

Matalas, N.C.:Statistical properties of tree ring data. Hydrol. Sci. J. 7, 39–47, 1962.

Matskovsky, V.V., Helama, S.: Testing long-term summer temperature reconstruction based on maximum density chronologies obtained by reanalysis of tree-ring data sets from northernmost Sweden and Finland. Clim.Past 10, 1473–1487, 2014.

Mencuccini, M., Martínez-Vilalta, J., Vanderklein, D., Hamid, H.A., Korakaki, E., Lee, S., Michiels, B.: Size-mediated ageing reduces vigour in trees. Ecology Letters, 8 (11), pp. 1183-1190, 2005.

Mitchell, V.L.: An investigation of certain aspects of tree growth rates in relation to climate in the central Canadian boreal forest. Technical report 33pp. Department of Meteorology, University of Wisconsin, 1967.

Pallardy, S.G.: Physiology of Woody Plants. Academic Press, 2010.

Panofsky, H.A., Brier, G.W.: Some applications of statistics to meteorology. University Park, Pennsylvania, p. 224, 1958.

Pena-Angulo, D., Cortesi, N., Brunetti, M., González-Hidalgo, J.C.: Spatial variability of maximum and minimum monthly temperature in Spain during 1981–2010 evaluated by correlation decay distance (CDD). Theoretical and Applied Climatology, 122 (1-2), pp. 35-45, 2015.

Peñuelas, J.: Plant physiology—a big issue for trees. Nature, 437:965–966, 2005.

Rinn, F.: TSAPWinTM – Time series analysis and presentation for dendrochronology and related applications, Version 4.69, 2005.

Ruiz, P.: Análisis dendroclimático de *Pinus uncinata Ramond* en la Sierra Cebollera (Sistema Ibérico). Cuadernos de Investigación Geográfica 15(1-2): 75-80, 1989.

Ruiz-Flaño, P.: Dendroclimatic series of Pinus uncinata R. in the Central Pyrenees and in the Iberian System. A comparative study. Pirineos 132:49–64, 1988.

Sánchez, E., Gallardo, C., Gaertner, M.A., Arribas, A., Castro, M.: Future climate extreme events in the Mediterranean simulated by a regional climate model: A first approach. Global and Planetary Change, 44 (1-4), pp. 163-180, 2004.

Saz, M.A.: Análisis de la evolución del clima en la mitad septentrional de España desde el siglo XV a partir de series dendroclimáticas. Servicio de Publicaciones de la Universidad de Zaragoza, Zaragoza, 1105 pp, 2003.

Schulman, E.: Dendroclimatic Changes in Semiarid America. Tucson, University of Arizona Press, pp. 142, 1956.

Smith, J. G. and Weston, H. K.: Nothing particular in this year's history, J. Oddball Res., 2, 14-15, 1954.

Smith, J. G. and Weston, H. K.: Nothing particular in this year's history, J. Oddball Res., 2, 14-15, 1954.

Stokes, M.A., Smiley, T.L.: An introduction to tree-ring dating, 2nd edn. The University of Arizona Press, Tucson, 1968.

Tejedor, E., de Luis, M., Cuadrat, J.M., Esper, J., Saz, M.Á.: Tree-ring-based drought reconstruction in the Iberian Range (east of Spain) since 1694. International Journal of Biometeorology, 12 p, 2015.

Vicente-Serrano, S.M. and Cuadrat, J.M.: North Atlantic oscillation control of droughts in north-east Spain: Evaluation since 1600 A.D. Climatic Change, 85 (3-4), pp. 357-379, 2007.

Wigley, T.M.L., Briffa, K., Jones, P.D.: On the average value of correlated time series, with applications in dendroclimatology and hydrometeorology.J Clim Appl Meteorol 23:201–213, 1984.

1 Table 1. Tree ring sites characteristics

Code	Site	Source	Lat	Long	Elevation	Species	Tree no	Sample no	Tree-rings	Period
s047	Urbión Covaleda	ITRDB	41.98	-2.87	1750	PISY	15	31	6549	1567-1983
s048	Urbión Duruelo	ITRDB	42.02	-2.90	1840	PISY	8	17	3590	1671-1983
s049	Urbión Quintenar	ITRDB	42.03	-3.03	1840	PISY	12	27	4713	1593-1985
s050	Urbión Vinuesa	ITRDB	42.00	-2.85	1750	PISY	4	8	1942	1681-1983
s006	Urbión	ITRDB	42.03	-2.7	1634	PISY	11	22	2397	1842-1977
CAV	Castillo de Vinuesa	UNIZAR	42.01	-2.75	1900	PIUN	18	36	9236	1593-2012
COV	Covaleda	IPE-CSIC-UNIZAR	41.93	-2.83	1500	PISY	16	48	14696	1568-1993
HER	Barranco de las heridas	IPE-CSIC-UNIZAR	41.94	-2.84	1500	PISY	25	32	9347	1562-1993
NEI	Neila	IPE-CSIC-UNIZAR	42.05	-3.08	1850	PISY	9	15	4822	1587-1992

URB	Picos de Urbión	UNIZAR	41.96	-2.82	1750	PISY	28	60	11328	1733-2012
VIN	Castillo de Vinuesa	IPE-CSIC-UNIZAR	42.03	-2.73	1900	PIUN	13	20	7653	1465-1992
						Total	159	316	76273	

UNIZAR University of Zaragoza, *IPE-CSIC* Spanish National Research Council, *ITRDB* International Tree-Ring Databank

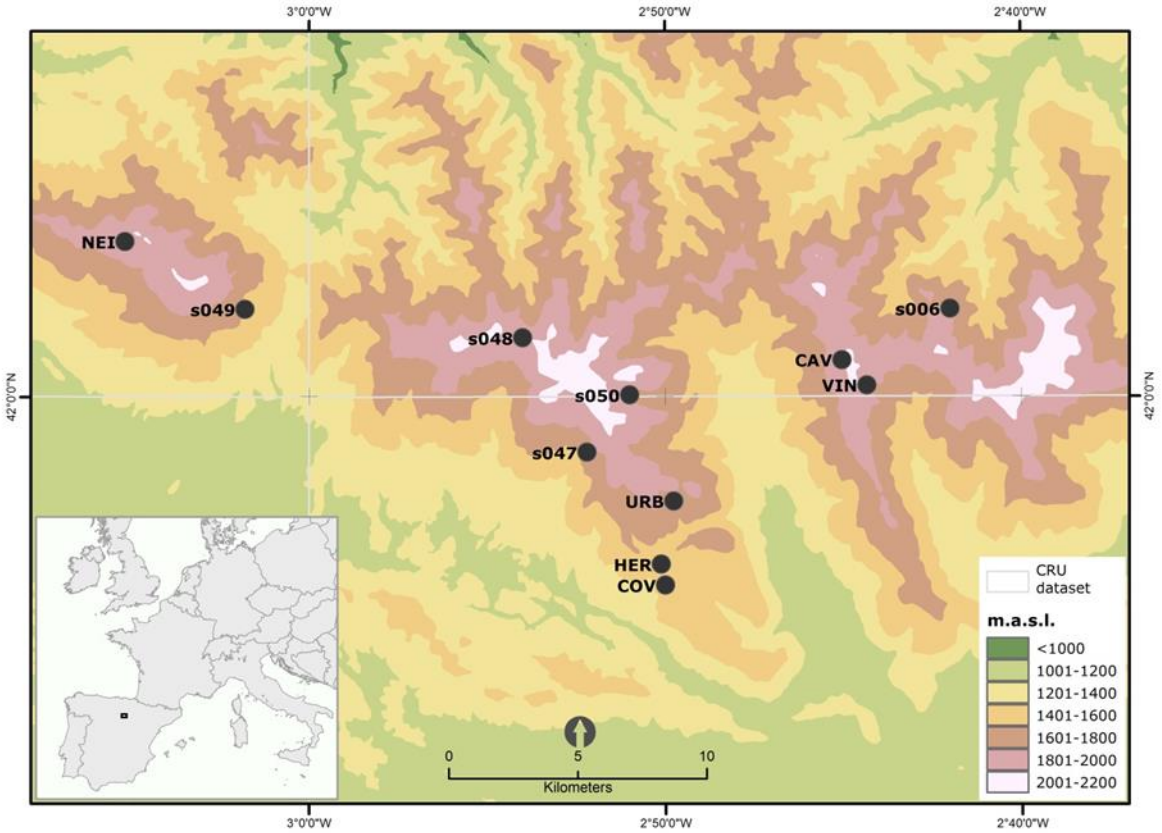

Figure 1. Map showing the tree ring study sites and the climate data (CRU TS v.3.22) grid points in the Western Iberian Range (Soria).

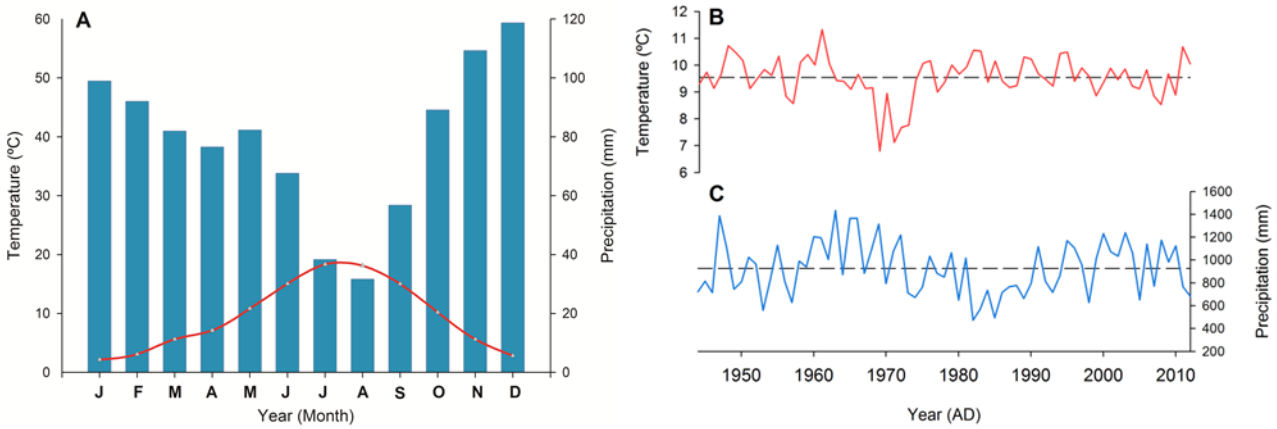

Figure 2. Climate diagram (A), mean temperature (B), mean precipitation (C) calculated using data from CRU TS v.3.22 over the period 1944-2012 (Harris et al 2014).

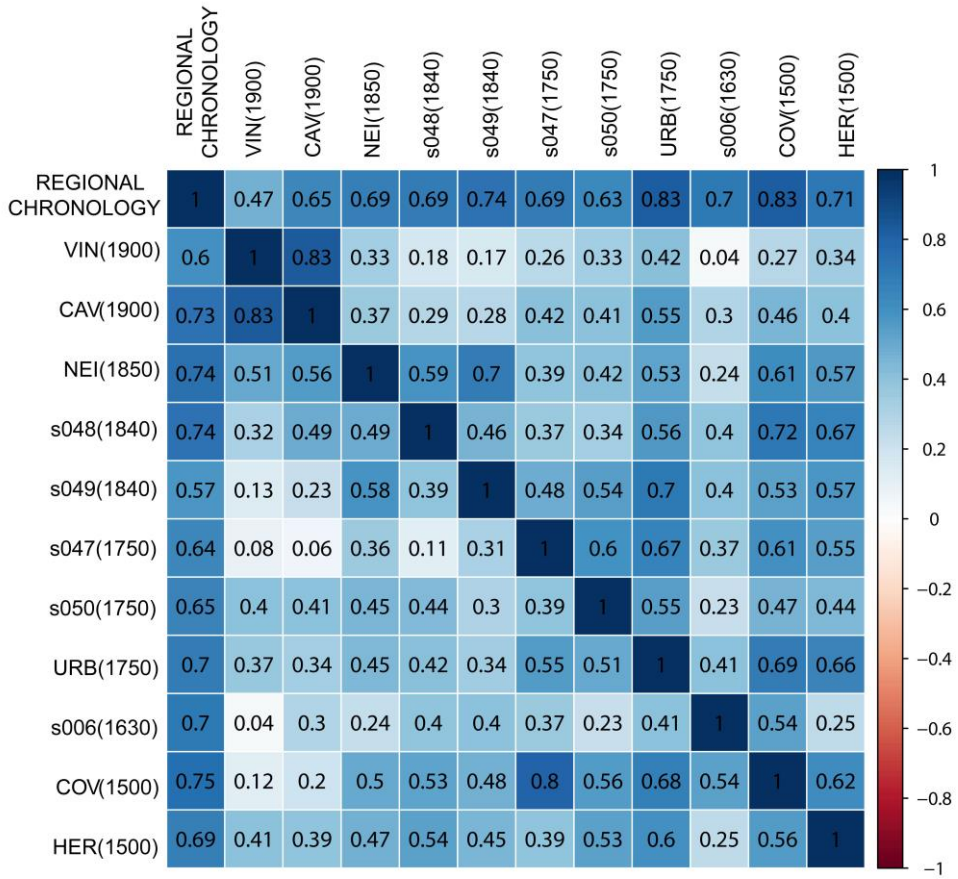

Figure 3. Inter correlation of the raw chronologies between sites and the regional chronology, sorted by elevation. Top right shows the correlations calculated over the common period

1842-1977. Bottom left shows the correlation over the full period of overlap between pairs of chronologies

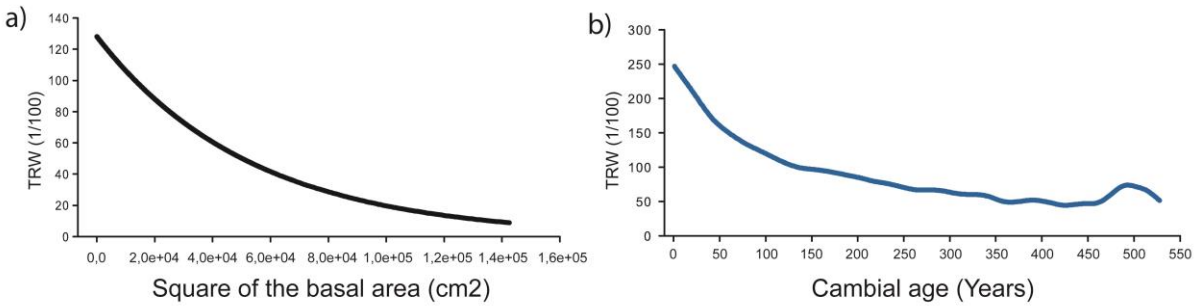

Figure 4. a) Represents the model of the BasPois method, b) represents the regional curve of the RCS method.

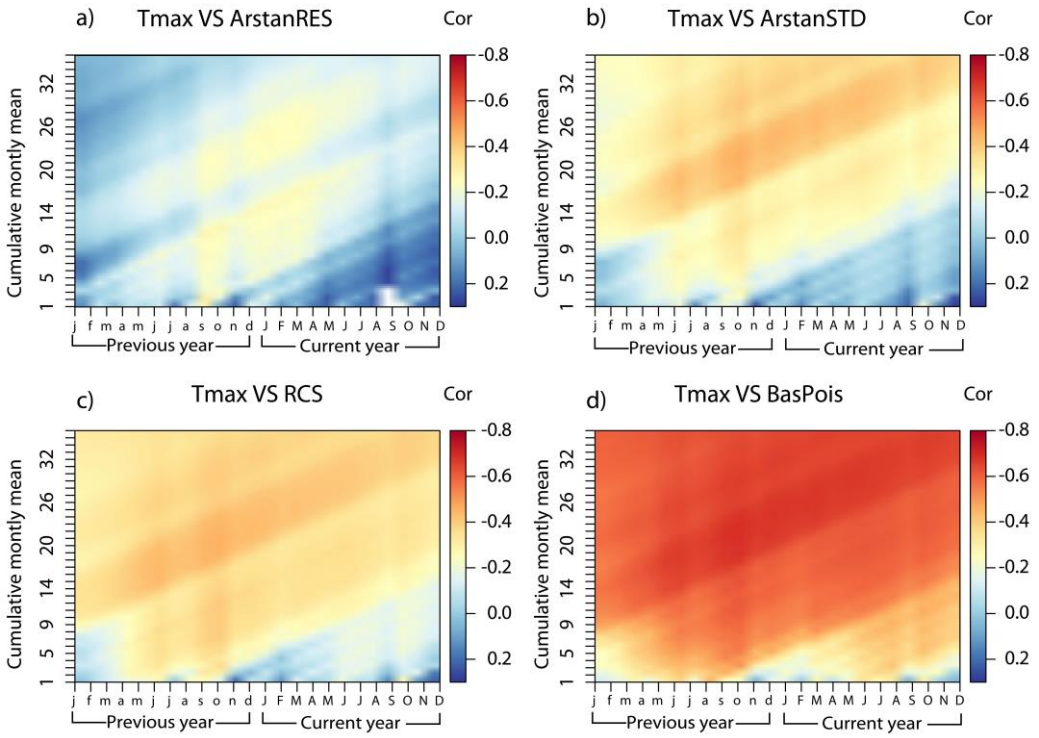

Figure 5. Correlation between the maximum temperature (from January of the previous year to December of the current year with a cumulative monthly mean from 1 to 36 months) and the residual Arstan chronology (a), the standard Arstan chronology (b), the RCS standard chronology (c) and the Basal Area-Poisson standard chronology (d).

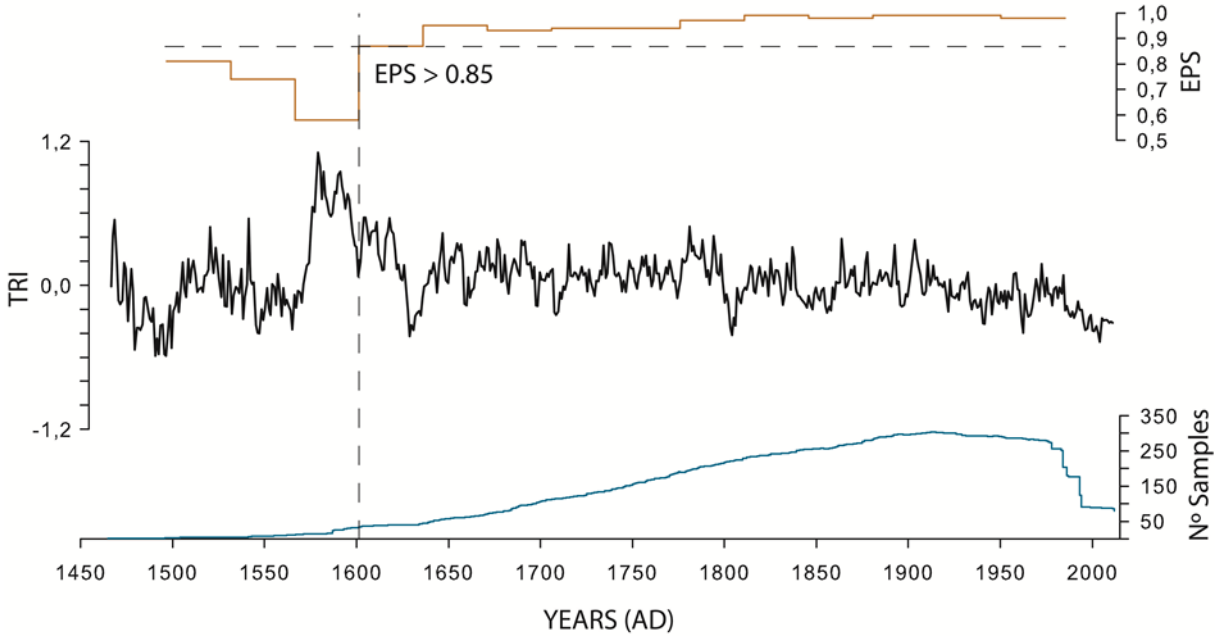

Figure 6. BasPois chronology (in black), number of samples (blue) and EPS statistic (computed over 30-y window lagged by 15 years) back to 1465. Vertical dashed line highlights the EPS=0.85 threshold in 1602.

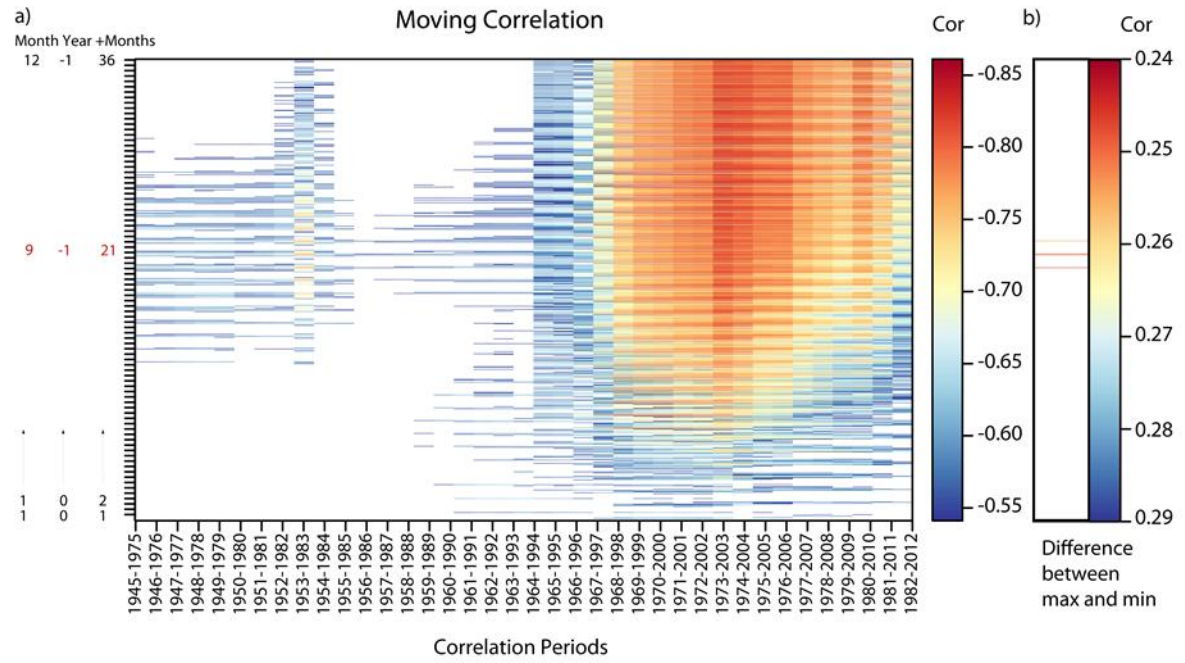

Figure 7.a) 30-year moving correlation from 1945 to 2012 between the maximum temperature, from January of the current year (1,0,1) to December of the previous year (12, -1, 36) with a cumulative monthly mean from 1 to 36 months and the BasPois chronology. Red numbers indicates the chosen climatological parameter; 9, September, -1, previous year, 21,

months used for the cumulative monthly mean. b) The four best parameters are represented. Reddish line indicates the least difference between the maximum and minimum correlation in the correlation periods.

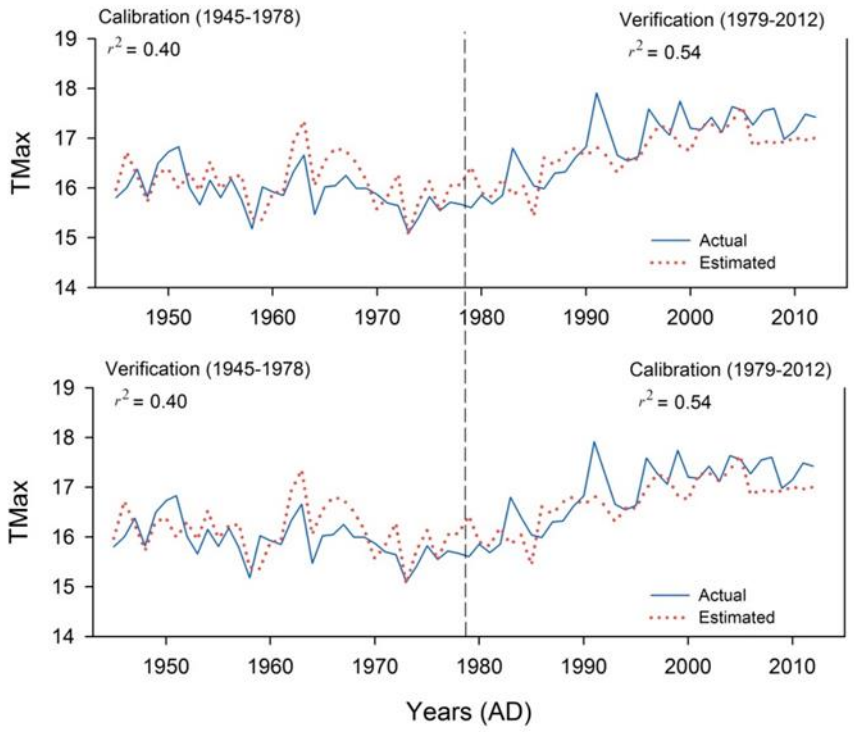

Figure 8. Calibration and verification results of the CRU data based $Tmax_{Sep\text{-}1}$ reconstruction

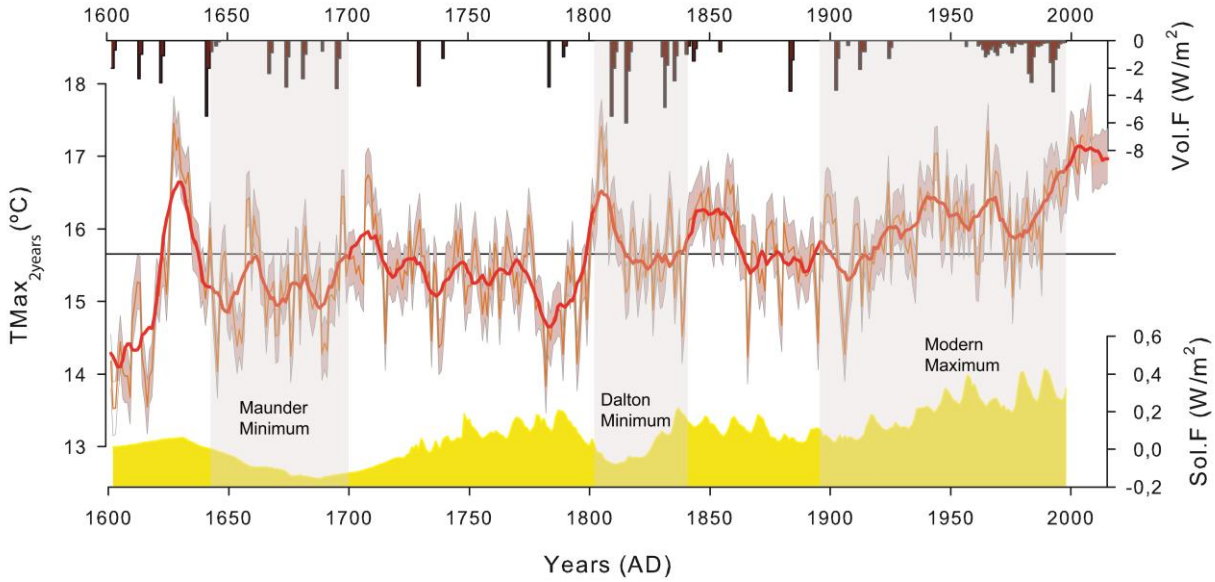

Figure 9. IR2T$_{max}$ reconstruction since AD 1602 for the Iberian Range. Bold red curve is a 11-year running mean, purple shading indicates the mean square error based on the calibration period correlation. Yellow shading at the bottom show solar forcing and bars on top indicate volcanic forcings (Crowley 2000).

	Calibration 1945-1978	Verification 1978-2012	Calibration 1979-2012	Verification 1945-1978	Period 1945-2012
Years	34	34	34	34	68
Correlation	-0.64	0.73	-0.74	0.64	-0.78
R^2	0.41	0.55	0.55	0.41	0.61
MSE	0.43	0.42	0.42	0.43	0.86
Reduction of error	0.40	0.65	0.65	0.40	0.56
Sing test	28+/6-	24+/10-	28+/6-	24+/10-	52+/16-
Durbin-Watson	1.31 p<0.01	1.53 p<0.05	1.53 p<0.05	1.31 p<0.01	1.45 p<0.001

Table 2. Calibration/verification statistics of the Tmax$_{Sep-1}$ reconstruction

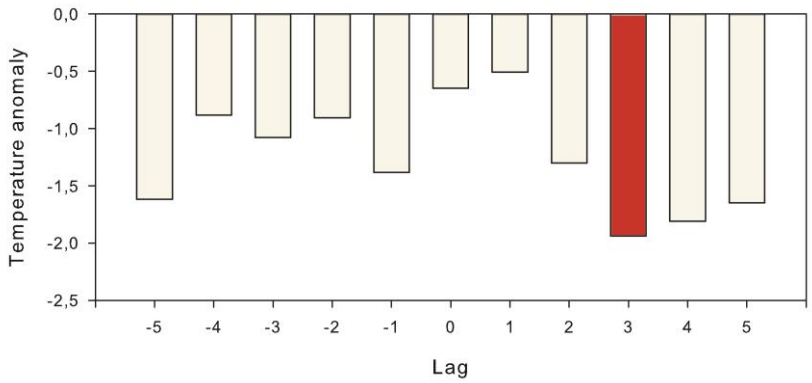

Figure 10. Superposed epoch analysis with a back and forward lag of 5 years. Significance ($p<0.05$) at 3 years after the extreme volcanic event.

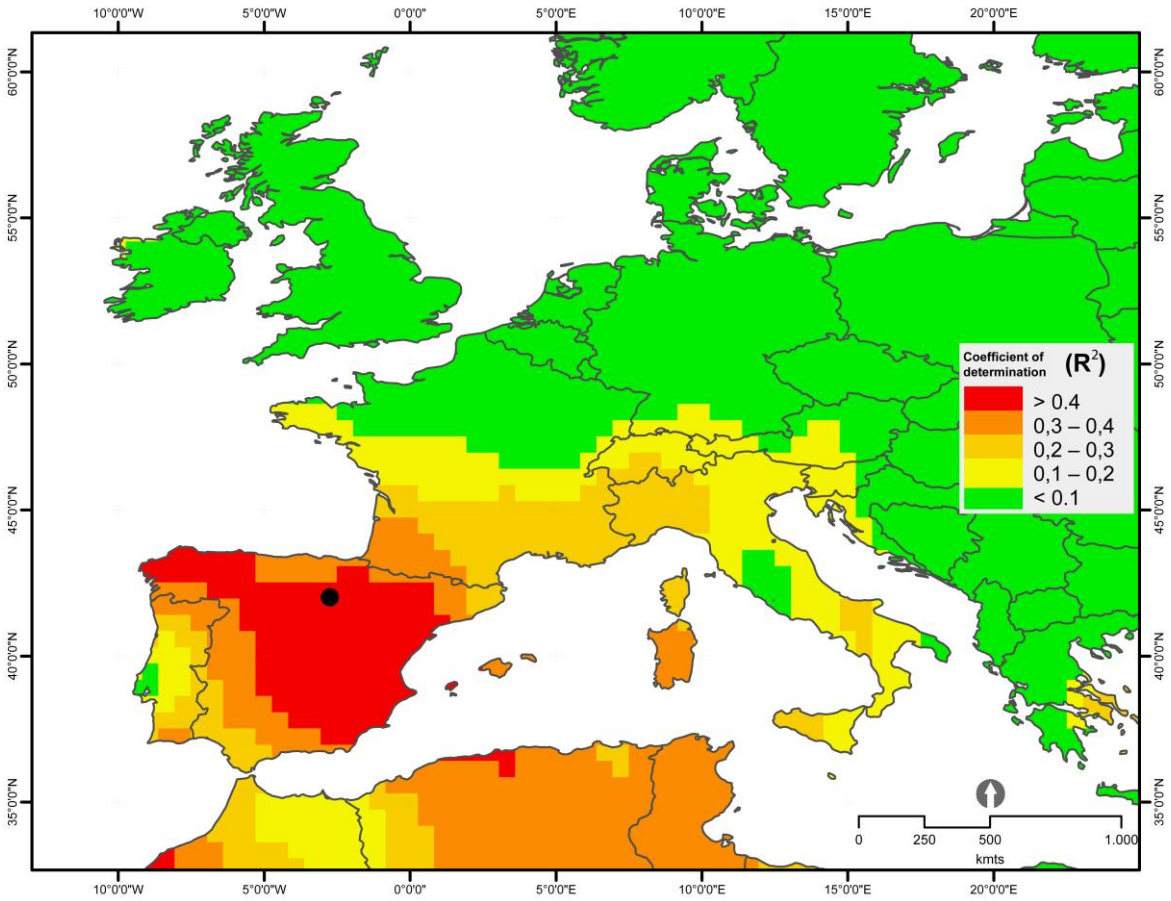

Figure 11. Map showing the spatial correlation patterns of the BasPois chronology with the gridded September of the previous year with a cumulative monthly mean of 21months data. Correlation values are significant at $p<0.0001$.